Thiophene-Phenylene and Thiophene-Thiazole Oligomeric Semiconductors with High Field-Effect Transistor On/Off Ratios

X. Michael Hong, Howard E. Katz,* Andrew J. Lovinger, Bo-Cheng Wang, and Krishnan Raghavachari

Bell Laboratories, Lucent Technologies, 600 Mountain Avenue, Room 1D-249, Murray Hill, New Jersey 07974

Received May 21, 2001. Revised Manuscript Received September 18, 2001

A series of thiophene-containing oligomers that are less electron rich than alpha-6T were synthesized, and the thin film morphologies and field-effect transistor characteristics of the oligomers were evaluated. Phenyl and thiazole rings were included in many of the oligomers, and a new synthesis of perfluoroalkylmethyl-terminated oligomers was developed. Desirably low off currents were associated with calculated highest occupied molecular orbital energies above ca. 5.0 eV relative to vacuum. Some of the oligomers displayed mobilities above 0.01 cm^2 $(Vs)^{-1}$, but there was no correlation of mobility with calculated orbital energies and some compounds with seemingly continuous morphologies had low mobilities nonetheless. One compound, 1,4-bis(5′-hexyl-2,2′-bithiophen-5-yl)benzene, showed promising behavior as a solution-deposited semiconductor, with mobility up to 0.02 cm^2 $(Vs)^{-1}$ and an on/off ratio up to 20 000.

Introduction

Organic semiconductors are of increasing interest for low-cost display drivers and logic elements. Field-effect transistors (FETs) with organic semiconductor channels have been fabricated in arrays to drive electrophoretic display pixels[1] and polymer-dispersed liquid crystals (http://www.research.philips.com/pressmedia/releases/000901a.html). Complementary logic elements and shift registers containing hundreds of organic-based FETs have been produced,[2] and high-speed organic circuits have been fabricated on polyester substrates.[3] The source and drain electrodes of individual FETs have been patterned using microcontact printing and inkjet methods[4] to give extraordinary aspect ratios. Inorganic[5] and hybrid[6] materials have been deposited as FET semiconductors using the methods of "organic electronics". Organic FET channels have been harnessed to demonstrate ambipolar transport,[7] chemical sensitivity,[8] superconductivity,[9] and electrically pumped lasers.[10]

Thiophene oligomers remain an important class of organic semiconductors for many applications and demonstrations. They are conveniently synthesized and processed and form highly aligned films when sublimed onto substrates. In a few instances, they can be deposited as high-mobility films from solution. One drawback to these compounds, however, is their relatively high energy (closeness to vacuum) for the highest occupied molecular orbital (HOMO), which leads to an apparent (and sometimes ill-defined) threshold voltage (V_t)[11] in the depletion regime (>0 for hole transporters). Figure 1 shows device characteristics for common organic FET semiconductors with depletion and accumulation mode V_t.

A depletion regime V_t occurs when there are enough mobile carriers (holes) in an FET at zero gate voltage to result in a device that is effectively on, and a significant extra voltage is needed to turn it off. For some applications, this is a severe drawback and can even outweigh a high mobility. The holes appear to arise from interactions between the semiconductor and oxygen (or some other oxidizing species), in the ambient environment or left over from the synthesis. It is possible for V_t to drift into the depletion regime over time as a pristine device becomes environmentally doped.

Some reports in the literature[12−15] suggest that a modest increase in the HOMO energy, as little as 0.3 eV, can greatly reduce the concentration of depletable carriers at zero gate voltage and provide a V_t on the accumulation side of zero (<0 for hole-transporting

---

* To whom correspondence should be addressed. E-mail: hek@bell-labs.com.

(1) Rogers, J.; Bao, Z.; Baldwin, K.; Dodabalapur, A.; Crone, B.; Raju, V. R.; Katz, H. E.; Kuck, V.; Amundson, K.; Jay Ewing, J.; Drziac, P. *Proc. Natl. Acad. Sci.* **2001**, *98*, 4835.

(2) Crone, B.; Dodabalapur, A.; Lin, Y. Y.; Filas, R. W.; Bao, Z.; LaDuca, A.; Sarpeshkar, R.; Katz, H. E.; Li, W. *Nature* **2000**, *403*, 521.

(3) Kane, M. G.; Campi, J.; Hammond, M. S.; Cuomo, F. P.; Greening, B.; Sheraw, C. D.; Nichols, J. A.; Gundlach, D. J.; Huang, J. R.; Kuo, C. C.; Jia, L.; Klauk, H.; Jackson, T. N. *IEEE Electron Device Lett.* **2000**, *21*, 534.

(4) Sirringhaus, H.; Kawase, T.; Friend, R. H.; Shimoda, T.; Inbasekaran, M.; Wu, W.; Woo, E. P. *Science* **2000**, *290*, 2123.

(5) Ridley, B. A.; Nivi, B.; Jacobson, J. M. *Science* **1999**, *286*, 746.

(6) Kagan, C. R.; Mitzi, D. B.; Dimitrakopoulos, C. D. *Science* **1999**, *286*, 945.

(7) Schon, J. H.; Berg, S.; Kloc, C.; Batlogg, B. *Science* **2000**, *287*, 1022.

(8) Torsi, L.; Dodabalapur, A.; Sabbatini, L.; Zambonin, P. G. *Sens. Actuators, B* **2000**, *67*, 312.

(9) Schon, J. H.; Kloc, C.; Batlogg, B. *Nature* **2000**, *406*, 702.

(10) Schon, J. H.; Kloc, C.; Dodabalapur, A.; Batlogg, B. *Science* **2000**, *289*, 599.

(11) Horowitz, G.; Hajlaoui, R.; Bouchriha, H.; Bourguiga, R.; Hajlaoui, M. *Adv. Mater.* **1998**, *10*, 923.

(12) Li, W.; Katz, H. E.; Lovinger, A. J.; Laquindanum, J. *Chem. Mater.* **1999**, *11*, 458.

(13) Aratani, S.; Kondo, K.; Ohara, S. U.S. Patent 5,854,139, 1998.

10.1021/cm010496z CCC: $20.00

Table 1. Compounds Synthesized for This Investigation

oligomer	metalloid[a]	condensation	solvent	% yield[b]
PTTP[25,26]	$B(OH)_2$	1 + 2 + 1	dimethoxyethane (aq bicarbonate)	90
PTTTP[25,26]	$B(OH)_2$	1 + 3 + 1	dimethoxyethane (aq bicarbonate)	95
PTTTTP[25,26]	$B(OH)_2$	1 + 4 + 1	dimethoxyethane (aq bicarbonate)	95
TTTTT[27]	$B(OH)_2$	1 + 3 + 1	dimethoxyethane (aq bicarbonate)	80
TTZTT	$SnBu_3$	1 + 3 + 1	toluene	60
TTPTT[28]	$B(OH)_2$	1 + 3 + 1	dimethoxyethane (aq bicarbonate)	95
2-dH-TTPTT	$SnBu_3$	2 + 1 + 2	toluene	10[c]
3-dH-TTPTT	$B(ONa)_2$	1 + 3 + 1	dimethoxyethane	70
PTPTP[29]	$B(OH)_2$	1 + 3 + 1	dimethoxyethane (aq bicarbonate)	90
PTZTP	$B(OH)_2$	1 + 3 + 1	dimethoxyethane (aq bicarbonate)	55
2-d(FCCH$_2$)-TTTTTT[d]	$SnBu_3$	2 + 2 + 2	toluene	50

[a] Group attached to end ring starting material coupling position. [b] Before vacuum sublimation. [c] Central ring starting material was 1,4-diiodobenzene. [d] FC = C_6F_{13} (compound **1**).

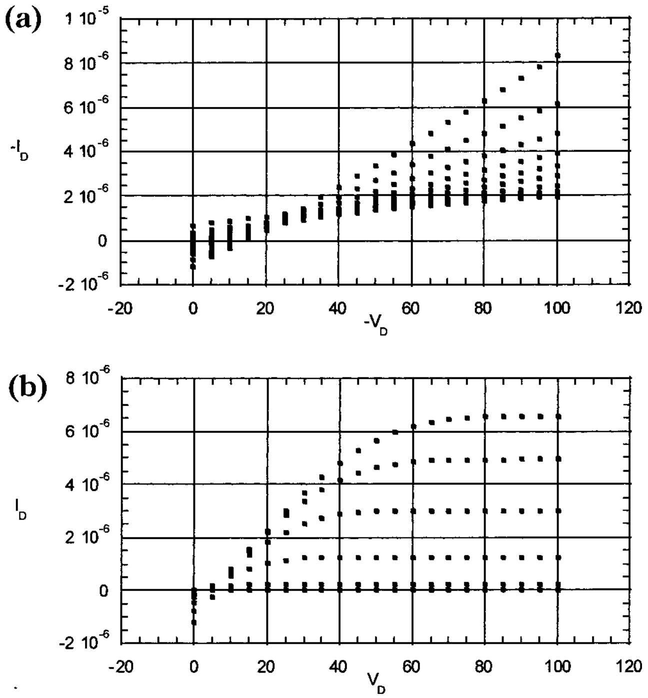

Figure 1. FET characteristics of (a) dihexyl-α-6T cast from chlorobenzene on polyimide and (b) bis(1*H*,1*H*-perfluorooctyl)-naphthalenetetracarboxylic diimide cast from trifluoromethylbenzene on SiO_2, showing depletion-mode threshold voltage (V_t) and accumulation mode V_t, respectively. The gate voltages (V_g) are changed in 20 V steps, from a minimum of 80 V in depletion (bottom of graph) to a maximum of 100 V in accumulation. Each curve indicates drain current vs drain voltage at a given V_g, although several of the depletion-region curves overlap. Note that only five curves in each graph are in the accumulation regime, although eight curves in Figure 1a show significant currents. The axis units are volts (abscissa) and amperes (ordinate).

FETs). In this work, we survey a variety of thiophene co-oligomers for their behavior as FET semiconductors. The HOMO energies were modulated by the introduction of phenylene and thiazolidene subunits, and in one case, a fluoroalkylmethyl end group. The syntheses are briefly described, devices are evaluated, and morphologies probed by X-ray diffraction (XRD) and transmission electron microscopy (TEM). Gradient-corrected density functional calculations are used to calculate molecular geometries and HOMO energies. There is little correlation between mobility and HOMO energy, although some correlations between mobility and morphology are determined. However, a strong correlation between the hole conductivity at zero gate voltage and the HOMO energy is uncovered. Finally, one compound is investigated for liquid-phase deposition.

Experimental Section

Oligomers were generally synthesized by coupling organometalloid derivatives of the terminal rings with the dibromide of a central subunit. The dibromo compounds were obtained by direct bromination with *N*-bromosuccinimide in dimethylformamide. Table 1 lists the prepared compounds, synthesis data, and references for the initial reports of compounds that had been previously synthesized. Structures of the oligomers synthesized for this study are shown below. The thiophene ring is abbreviated to T, the phenyl(ene) to P, and thiazole to Z; 2-dH refers to hexyl substituents at the terminal carbons adjacent to sulfur, while 3-dH refers to hexyl substituents at the terminal carbons not adjacent to sulfur. $Pd(PPh_3)_4$ was used as catalyst in every case. All compounds were purified

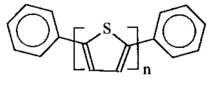

PTTP, n = 2
PTTTP, n = 3
PTTTTP, n = 4

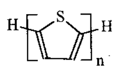

TTTTT, n = 5
TTTTTT, n = 6

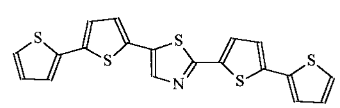

TTZTT

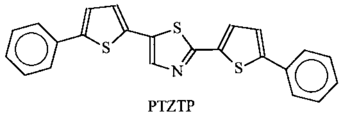

PTZTP

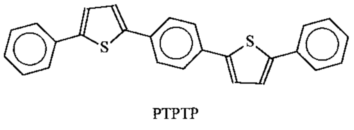

PTPTP

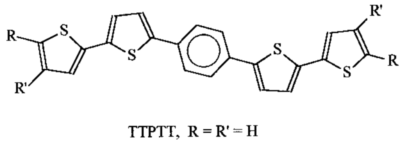

TTPTT, R = R' = H
2-dH-TTPTT, R = C_6H_{13}
3-dH-TTPTT, R' = C_6H_{13}

---

(14) Hajlaoui, R.; Horowitz, G.; Garnier, F.; ArceBrouchet, A.; Laigre, L.; ElKassmi, A.; Demanze, F.; Kouki, F. *Adv. Mater.* **1997**, *9*, 389.

(15) Gundlach, D. J.; Lin, Y. Y.; Jackson, T. N.; Schlom, D. G. *Appl. Phys. Lett.* **1997**, *71*, 3853.

Table 2. FET Characteristics of Oligomeric Semiconductors

compound	mobility[a] (cm^2 $(Vs)^{-1}$)	off current (nA)[b]	on/off ratio	V_t (V)[b]
PTTP	0.0065 (0.0014)	0.5	10^4 (1000)	−12
PTTTP	0.0006 (0.003)	8	70 (4000)	0
PTTTTP	0.014 (0.033)	5	2000 (1700)	−9
TTTTT	0.0057	4	800	−4
TTZTT	0.000 06 (0.007)	0.3	160 (10^4)	−7
TTPTT	0.000 05 (0.0005)	0.5	140 (590)	+27
2-dH-TTPTT	0.02	5	4000	−15
3-dH-TTPTT	(0.000 04)	0.4	10	−46
PTPTP	0.02 (0.04)	0.3	5×10^4 (8×10^4)	−13
PTZTP	0.0001	0.6	80	−23
TTTTTT	0.02[30]	4	10^3−10^4	0[31]
2-dH-TTTTT	0.03 (0.1)[12]	5	10^3−10^4	+10[12]
2-d($FCCH_2$)-TTTTTT	inactive			

[a] Values in parentheses were obtained on films deposited at 60−80 °C. [b] Films deposited at ambient temperature.

Table 3. Calculated Properties of Oligomeric Semiconductors Listed in Order of Increasing HOMO Energies (in eV)

compound	HOMO (B3-LYP/6-31G*)	LUMO (B3-LYP/6-31G*)	HOMO−LUMO gap (B3LYP/6-31G*)
2-dH-TTTTT	−4.75	−1.94	2.81
TTTTTT	−4.80	−2.18	2.62
TTTTT	−4.86	−2.08	2.78
PTTTTP	−4.87	−2.03	2.84
2-dH-TTPTT	−4.90	−1.77	3.13
PTTTP	−4.95	−1.90	3.05
3-dH-TTPTT	**−4.97**	**−1.82**	**3.15**
TTZTT	**−5.05**	**−2.22**	**2.83**
TTPTT	**−5.07**	**−1.86**	**3.21**
PTTP	**−5.13**	**−1.67**	**3.46**
PTZTP	**−5.13**	**−2.14**	**2.99**
PTPTP	**−5.16**	**−1.69**	**3.47**

Table 4. Layer Spacings of Sublimed Oligomer Films

compound	spacing (X-ray, Å)	orders obsd	calcd length[f] (Å)
PTTP	17	1, 2, 4	17.0
PTTTP	20.5	1, 2, 5[a]	20.8
PTTTTP	22.5, 24[b]	1−2	24.7
TTTTT	20.5	1−2	20.3
TTZTT	20.5	1−5	20.2
TTPTT	20	1−5[c]	20.6
2-dH-TTPTT	34	1−2	34.0
3-dH-TTPTT	35	1, 2, 4[d]	34.0
PTPTP	22	1−6	21.1
PTZTP	20.5	1−5	20.6
TTTTTT	23[32]	1−6	24.2
2-dH-TTTTT	31	1−2	33.4
2-d($FCCH_2$)-TTTTTT[d]	34	1−3[e]	

[a] Third, fourth, and sixth orders very weak. [b] Two polymorphs observed with deposition on room-temperature substrate. [c] Distinct polymorph observed with deposition on high-temperature substrate. [d] First order observed weakly, from solid flakes only. Second order strong. [e] Substrate 115 °C. Polymorphic. Ambient-temperature substrate gave much less crystalline film. [f] Calculated distance between the farthest atoms at the B3LYP/6-31G* level of theory.

after isolation as crude solids by vacuum sublimation. Soluble compounds were examined by NMR, and the new compounds were assayed by elemental analysis.

FETs were fabricated and evaluated as previously described (except for liquid-phase deposition), using 500 Angstrom-thick unpatterned semiconductor films and top gold contacts (width/length was 18) on 3000 Angstrom-thick SiO_2 dielectrics grown on doped silicon substrates that were a few cm^2 in area.[16] Liquid-phase deposition was done at 80−110 °C, and carbon paste top contacts were generally used for source and drain. TEM and XRD were performed as before.[12]

Theoretical Section

Electronic structure calculations were carried out using the Gaussian 98 program package. The structures of all the compounds were determined by complete geometry optimization using the gradient-corrected B3LYP density functional with the polarized 6-31G* basis set (B3LYP/6-31G*).[17] The calculated HOMO and lowest unoccupied molecular orbital (LUMO) energies are listed along with the associated band gap in Table 3. The calculated molecular lengths (the distances between the farthest atoms) are listed in the last column of Table 4.

Synthesis

5-dH-TTPTT was synthesized using 1,4-diiodobenzene. The yield was much lower than that of an analogous coupling with 1,4-dibromobenzene used to synthesize 2′,2‴-dibutyl-TTPTT for another purpose, although analytically pure material was eventually obtained. The iodo groups were found to undergo side reactions more rapidly than the desired coupling.

The synthetic sequence for $C_6F_{13}CH_2TTTTTTCH_2C_6F_{13}$ (**1**) is shown in Scheme 1. Coupling[18] of the aldehyde **2** was efficient to form hydroxy compound **3**, and could probably be further optimized by adjusting the excess of reagents and other reaction conditions. The coupling was also successful using thiophene-3-carboxaldehyde. Numerous reagents were then examined for the reduction of **3** to **4**, including phosphines and borohydrides. While these gave either no reaction or decomposition, $Me_3SiCl/NaI/MeCN$[19,20] gave extremely clean reduction, with yields exceeding 90%. Interestingly, the reduction of the corresponding 3-thienyl hydroxy compound was completely unsuccessful; a batch of silyl iodide reagent was divided into two portions and shown to reduce **3** while leaving the 3-thienyl compound untouched under identical conditions. The reduction must therefore proceed via a resonance-stabilized carbocation-like transition state. Bromination of **4** gave **5** cleanly but was sluggish after 80% conversion. Addition of excess bromine led to overbromination.

---

[16] Laquindanum, J.; Katz, H. E.; Lovinger, A. J. *J. Am. Chem. Soc.* **1998**, *120*, 664.

[17] Frisch, M. J. *GAUSSIAN 98*; Gaussian, Inc.: Pittsburgh, PA, 1998.

[18] Gassman, P. G.; Oreilly, N. J. *J. Org. Chem.* **1987**, *52*, 2481.

[19] Sakai, T.; Miyata, K.; Tsuboi, S.; Takeda, A.; Utaka, M.; Torii, S. *Bull. Chem. Soc. Jpn.* **1989**, *62*, 3537.

[20] Stoner, E. J.; Cothron, D. A.; Balmer, M. K.; Roden, B. A. *Tetrahedron* **1995**, *51*, 11043.

Scheme 1. Synthesis of d-(FC−CH$_2$)-TTTTTT

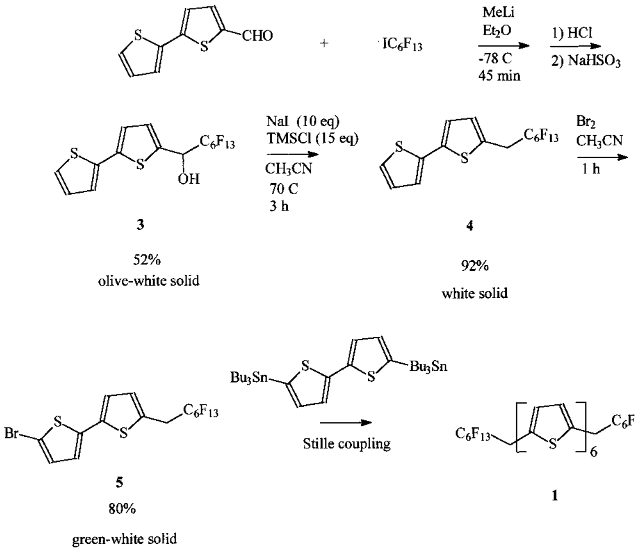

Compound **5** was triturated with MeOH and used along with <20% of **4** as an impurity in the coupling with bis(tributylstannyl)bithiophene. The yield was comparable to that obtained from analogous Stille couplings,[12,21] although more homocoupling than typical was observed. A satisfactory elemental analysis for **1** was obtained after trituration with hot xylene and sublimation at 10^{-4} Torr. The compound is light orange, extremely hydrophobic, and virtually insoluble.

FET Characteristics

Table 2 lists mobilities, off currents, on/off ratios, and threshold voltages for compounds prepared during this study and also for two other semiconductors previously described in the literature. Insertion of the non-thiophene rings is generally effective in bringing V_t into the accumulation regime. No special attempt was made to purify any of the compounds beyond a single vacuum sublimation or to protect the device surfaces from the ambient environment before or after fabrication.

Results of the density functional calculations are listed in Table 3. There is a general grouping of semiconductors with relatively less negative HOMO energies associated with higher off currents and another group with more negative (more stable) HOMOs and lower off currents, as shown in Figure 2. To illustrate this point clearly, the oligomers are listed in order of increasing HOMO energies in Table 3. However, there is no particular correlation between mobility and HOMO energy for this set of semiconductors.

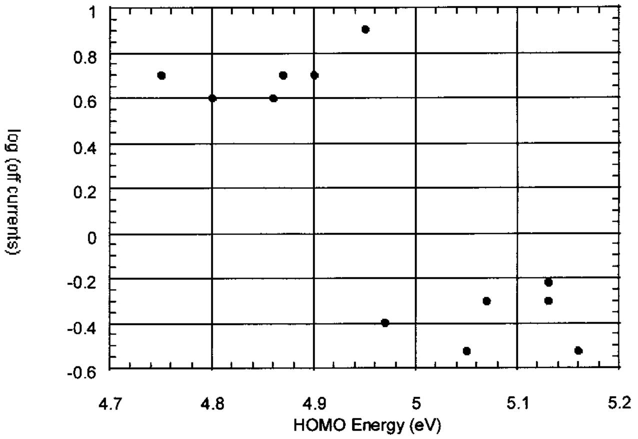

Figure 2. Logarithms of FET off currents plotted against calculated HOMO energies of various semiconductors. The points that are read from the left to the right in the figure correspond to semiconductors in Table 3 listed from the top to the bottom. The points in the lower right part of the figure (higher HOMO energies, lower off currents) are listed in **bold** in Table 3. The zero value of log(off current) corresponds to 1 nA.

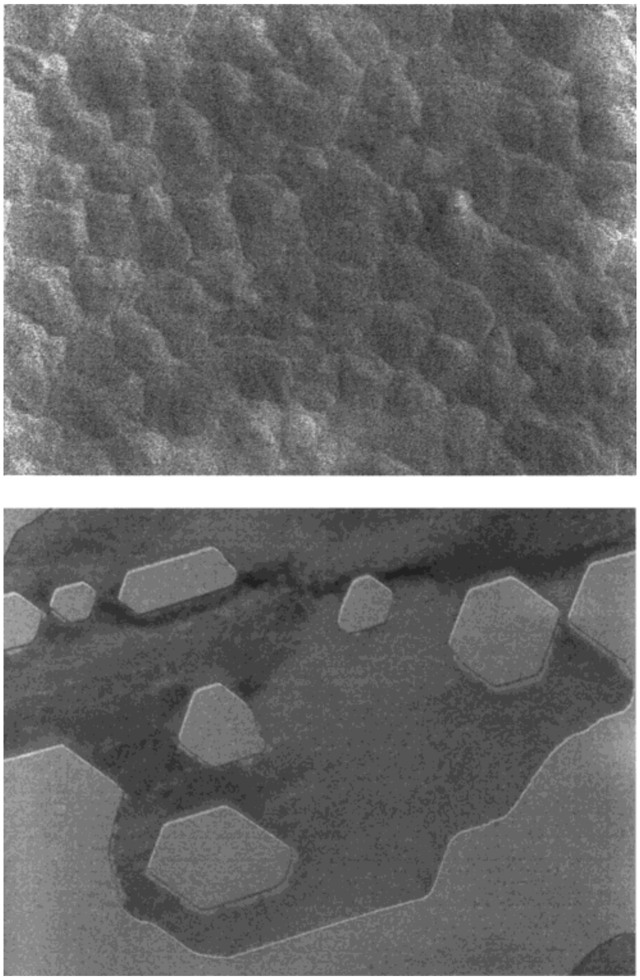

Figure 3. Electron micrographs of (a) PTTTP sublimed onto an ambient-temperature substrate and (b) PTTP sublimed onto a 60 °C substrate.

In Table 4, the layer spacings determined by XRD, the number of observed orders, and the molecular lengths derived from the density functional calculations are tabulated. The agreement between observed and expected spacings is striking and shows once again that nearly perpendicular molecular orientation and layer planes parallel to the substrate surface are almost universally observed. Figure 3 shows representative morphologies obtained by electron microscopy. Unlike most of the compounds discussed below, the 3-dH compound film appeared rough by *optical* microscopy, on the 1−10 μm scale.

The morphology of all of these materials varies from extremely large and regular crystals to randomly shaped

---

(21) Katz, H. E.; Laquindanum, J. G.; Lovinger, A. J. *Chem. Mater.* **1998**, *10*, 633.

Table 5. Device Characteristics of FETs with 2-dH-TTPTT as Semiconductor

dielectric	semiconductor deposition (ppm, solvent)	mobility (cm^2 (Vs)$^{-1}$)	on/off ratio
SiO$_2$	sublimation	0.02	4000
PMMA[a]	sublimation	0.001	30
SiO$_2$	400, xylene	0.02	600
PMMA[a]	400, xylene	0.005	1200
PMMA[a]	200, chlorobenzene	0.005−0.02	5000−20 000
glass resin	100, xylene	0.01	2200
glass resin	50, 1,2-dichloroethane	0.02[c]	7000
glass resin	50, toluene[b]	0.001−0.002	8−10

[a] 10% hydroxyethyl methacrylate copolymer cross-linked with 4,4′-methylenebis(phenyl isocyanate). [b] No heating of solution or substrate during deposition; solution was pooled in a depression and applied/dried three times. Active area 0.5 cm^2. [c] Best device of a heterogeneous set.

nanocrystallites depending upon the material itself and the temperature of the substrate. For room-temperature deposition, the crystals were of the order of 50−200 nm for most compounds; the morphology for PTTTP shown in Figure 3a is typical. Generally, the crystals for Z-containing materials (e.g., PTZTP and TTZTT) were smaller and more disordered than that for those containing only T and P units. On the other hand, PTTP consisted of regular μm-sized crystals even at room temperature.

Deposition at higher temperatures generally yielded highly regular crystals, exhibiting distinct crystallographic faceting and extending to many micrometers. PTTP is remarkable in that it self-anneals at the deposition temperature of 60 °C, forming the striking crystallographically bounded holes seen in Figure 3b. Examination of the single-crystal patterns from all of these materials shows that they all pack with essentially the same projected rectangular unit cell having $a = 0.75-0.76$ and $b = 0.56-0.57$ nm. This isomorphism is remarkable in view of the different chemical groups and molecular lengths represented among these compounds.

The compound 2-dH-TTPTT was particularly advantageous in its morphology, mobility, on/off ratio, threshold voltage, and solubility. It could be deposited effectively from a variety of solvents as well as by sublimation, and a variety of dielectric substrates could be used. Properties of devices made with this semiconductor are delineated in Table 5, and representative $I-V$ plots are displayed in Figure 4. Mobilities ranged from 0.001 to 0.02 cm^2 (Vs)$^{-1}$. The on/off ratio was >1000 for several kinds of devices made from both sublimed and solution-deposited films. Active areas up to 2 cm^2 were attained, and polymer dielectrics (for example, poly(methyl methacrylate) with 10% urethane cross-links and glass resin 720P obtained from Techneglas) could be used. Unpatterned bottom contact devices had lower on/off ratios than top contact devices on the same substrate, as previously observed with other semiconductors such as copper phthalocyanine. The use of the less toxic xylene as solvent instead of chlorinated solvents is attractive. The use of unheated toluene solution as a deposition vehicle shows that an unheated process is conceivable but may be less convenient and may not produce a film quality as high as processes involving heated solutions and/or substrates.

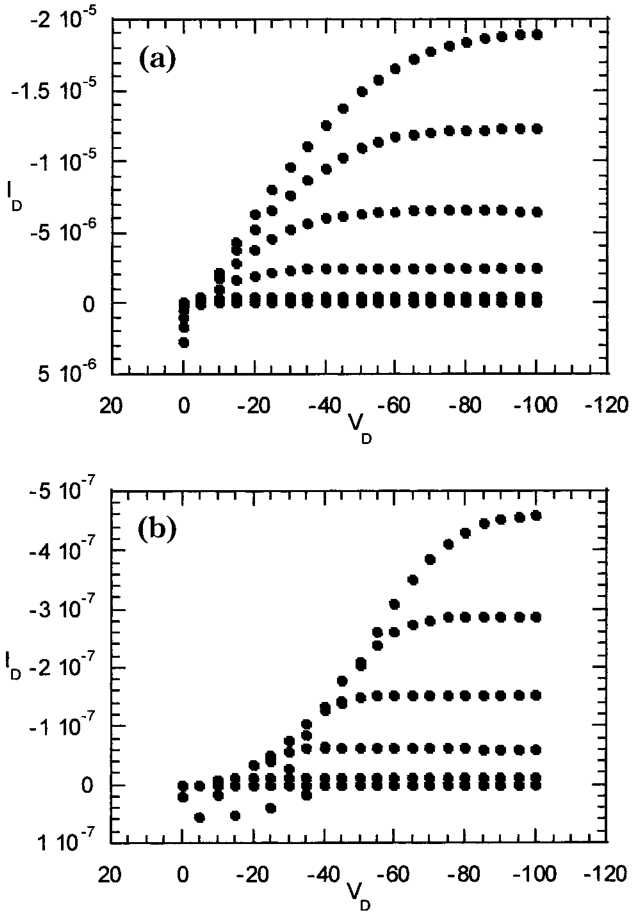

Figure 4. FET characteristics for 2-dH-TTPTT (a) sublimed onto SiO$_2$/Si with gold top contacts and (b) cast from 100 ppm xylene solution on a glass resin surface within a 2 cm^2 rectangle defined by the fluorinated polymer 3M-722. The solution was applied at room temperature to a substrate heated at 100 °C. Part of the rectangle had gold bottom contacts. The entire area of the rectangle contained active semiconductor. Top contact carbon electrodes were applied to a region that did not have gold contacts, and those device characteristics are pictured. Both the gate capacitance and width/length ratio were lower than those for the sublimed device. When bottom contact gold was used, the apparent mobility was an order of magnitude lower because of graininess near the contacts. The gate voltages and units are as for Figure 1.

Discussion

The data obtained and reported here are consistent with a model of ambient on/off ratio being determined by several factors including the HOMO energy level and the semiconductor morphology. Many of the high on/off ratio semiconductors combine relatively more stable (less easily oxidizable) HOMOs with interconnected, continuous morphologies. The stabilization of the HOMO (or destabilization of the hole) can be a result of the introduction of less electron donating subunits, such as the thiazole ring, or a decrease in planarity, such as when heterocycle−heterocycle linkages are replaced with bonds to phenyl rings. Some of the low on/off ratios are associated with obviously discontinuous morphology or less stable HOMOs, while others remain mysterious. Perhaps some unfavorable interaction with the dielectric surface, a trapping impurity, or a degree of grain isolation undetectable by electron microscopy is responsible.

The off current is determined by the number of carriers present in the zero gate device and the mobility of those carriers. The on current is produced by the capacitive injection of additional carriers by the gate and is determined by the mobility of those particular carriers. Since all of the devices considered here had the same channel dimensions, dielectric properties, and semiconductor film thicknesses, the on/off ratios track inversely with the original carrier density and positively with the ratio of the high voltage to zero voltage mobility. These parameters are influenced strongly by the HOMO energy, because carriers are less likely to be produced in a less easily oxidized compound, and those carriers are more likely to be trapped. However, the absolute high voltage mobility is little affected by the HOMO energy. Single-crystal data[22] as well as numerous thin film precedents indicate a convergence of mobilities to a common order of magnitude among compounds with the typical herringbone solid state packing and continuous morphologies, even though HOMO levels may differ by as much as 0.5 eV. Furthermore, thin film mobilities have been shown, by conducting probe atomic force microscopy, to be limited almost entirely by grain boundary resistances and contact effects[23] rather than carrier transport within the crystalline bulk.

Similar considerations apply to *n*-channel semiconductors but with electrons rather than holes as charge carriers. For example, NTCDIs and also a recently reported fluorocarbon-substituted sexithiophene[24] have higher LUMO energy levels (less stable electrons and more difficult reduction) than tetracyanonaphthoquinodimethane and consequently much higher on/off ratios.

Conclusion

Thiophene, phenylene, and thiazole rings may be linked in a variety of sequences and lengths to produce semiconducting molecular frameworks. Molecular designs where the HOMO is stabilized increase the probability that a high on/off ratio can be obtained. The mobilities, however, are not well-correlated with the HOMO energies and instead depend on morphological factors that are not entirely apparent. Morphological improvements could likely be obtained by varying the end substituents and optimizing deposition temperatures, neither of which were extensively done here. The smaller conjugated units, particularly the exceedingly simple and readily available PTTP, are suitable for vapor deposition under moderate conditions of temperature and vacuum. In the most favorable cases, liquid-phase deposition is enabled. Additional improvements in the on/off ratio can be gained by isolating the devices through semiconductor patterning.

One other beneficial effect of the stabilized HOMO can be a threshold voltage decidedly in accumulation. This affords the opportunity to selectively adjust the threshold voltage of some devices to zero or even into the depletion regime, thereby realizing memory elements and tuned or adaptable circuits. This process will be described in a forthcoming publication.[33]

Acknowledgment. We thank Bao, Z., Dobalapur, A., Rogers, J. A., and Li, W. for valuable discussions.

CM010496Z

---

(22) Schon, J. H.; Berg, S.; Kloc, C.; Batlogg, B. *Mater. Res. Soc. Symp. Proc.* **2000**, *598*, BB9.5.1.

(23) (a) Chwang, A. B.; Frisbie, C. D. *J. Phys. Chem. B* **2000**, *104*, 12202. (b) Chwang, A. B.; Frisbie, C. D. *J. Appl. Phys.* **2001**, *90*, 1342.

(24) Facchetti, A.; Deng, Y.; Wang, A.; Koide, Y.; Sirringhaus, H.; Marks, T. J.; Friend, R. H. *Angew. Chem., Int. Ed.* **2000**, *39*, 4547.

(25) Hotta, S.; Lee, S. A. *Synth. Met.* **1999**, *101*, 551.

(26) Hotta, S.; Lee, S. A.; Tamaki, T. *J. Heterocycl. Chem.* **2000**, *37*, 25.

(27) Hajlaoui, R.; Horowitz, G.; Garnier, F. *Adv. Mater.* **1997**, *9*, 389.

(28) Sato, T.; Hori, K.; Fujitsuka, M.; Watanabe, A.; Ito, O.; Tanaka, K. *J. Chem. Soc., Faraday Trans.* **1998**, *94*, 2355.

(29) Hotta, S.; Kimura, H.; Lee, S. A.; Tamaki, T. *J. Heterocycl. Chem.* **2000**, *37*, 281.

(30) Katz, H. E.; Torsi, L.; Dodabalapur, A. *Chem. Mater.* **1995**, *7*, 2235.

(31) Horowitz, G.; Fichou, D.; Peng, X. Z.; Garnier, F. *Synth. Met.* **1991**, *41*, 1127.

(32) Lovinger, A. J.; Davis, D. D.; Ruel, R.; Torsi, L.; Dodabalapur, A.; Katz, H. E. *J. Mater. Res.* **1995**, *10*, 2958.

(33) Katz, H. E.; Hong, X. M.; Dodabalapur, A.; Sarpeshkar, R. *J. Appl. Phys.*, in press.